COMENIUS UNIVERSITY IN BRATISLAVA

FACULTY OF MATHEMATICS, PHYSICS AND INFORMATICS

MODELLING IMMUNE RESPONSE TO VIRAL INFECTION

2012 **Lenka MATEJOVIČOVÁ**

COMENIUS UNIVERSITY IN BRATISLAVA
FACULTY OF MATHEMATICS, PHYSICS AND INFORMATICS
DEPARTMENT OF APPLIED MATHEMATICS AND STATISTICS

MODELLING IMMUNE RESPONSE TO VIRAL INFECTION

BACHELOR'S THESIS

Study programme:	Economic and Financial Mathematics
Branch of study:	1114 Applied Mathematics
Supervisor:	Mgr. Katarína Boďová, PhD.

Bratislava 2012

Lenka MATEJOVIČOVÁ

UNIVERZITA KOMENSKÉHO V BRATISLAVE
FAKULTA MATEMATIKY, FYZIKY A INFORMATIKY
ODDELENIE APLIKOVANEJ MATEMATIKY A ŠTATISTIKY

MODELOVANIE IMUNITNEJ ODPOVEDE NA VÍRUSOVÚ INFEKCIU

BAKALÁRSKA PRÁCA

Študijný program:	Ekonomická a finančná matematika
Študijný odbor:	1114 Aplikovaná matematika
Vedúci práce:	Mgr. Katarína Boďová, PhD.

Bratislava 2012

Lenka MATEJOVIČOVÁ

Univerzita Komenského v Bratislave
Fakulta matematiky, fyziky a informatiky

ZADANIE ZÁVEREČNEJ PRÁCE

Meno a priezvisko študenta: Lenka Matejovičová
Študijný program: ekonomická a finančná matematika (Jednoodborové štúdium, bakalársky I. st., denná forma)
Študijný odbor: 9.1.9. aplikovaná matematika
Typ záverečnej práce: bakalárska
Jazyk záverečnej práce: anglický

Názov: Modelling Immune Response to Viral Infection

Cieľ: Analysis and reduction of a mathematical model of immune response.

Anotácia: The mammalian immune response to viral infection is governed by complicated chemical processes, consisting of an activation of multiple signal molecules and their further effects on the system. The goal of this work is to gain understanding of the relationship between different parts of the system using both numerical and analytical tools and use it to simplify existing reaction-based models.

Vedúci: Mgr. Katarína Boďová, PhD.

Dátum zadania: 16.10.2011

Dátum schválenia: 27.10.2011

doc. RNDr. Margaréta Halická, CSc.
garant študijného programu

.....
študent

.....
vedúci

Acknowledgements

In the first place I would like to express thanks to my supervisor Mgr. Katarína Boďová, PhD. for the support and guidance she offered me throughout the elaboration of this thesis.

My special thanks goes to Simon D. W. Frost, M. A., D. Phil. for his support and advice while being my supervisor during the Amgen Scholarship Programme at the Department of Veterinary Medicine in Cambridge, where the related project was realised, giving rise to the idea of this work.

Last, but not least, I would like to thank my family and friends for their support and patience .

Declaration on Word of Honour

I declare on my honour that this thesis was written on my own, with the only help provided by my supervisors and the referred-to literature and sources.

In Bratislava June 1, 2012

.....

Lenka Matejovičová

Abstrakt

MATEJOVIČOVÁ, Lenka: Modelovanie imunitnej odpovede na vírusovú infekciu, [Bakalárska práca], Univerzita Komenského v Bratislave, Fakulta matematiky, fyziky a informatiky, Katedra aplikovanej matematiky a štatistiky, vedúci práce: Mgr. Katarína Boďová, PhD., Bratislava, 2012, 42s.

Koevolúcia patogénov a ich hostiteľov viedla k vývoju mnohých imunitných mechanizmov, ktoré sú schopné rozoznávať molekulárne štruktúry typické pre patogény. Jedna z takých molekúl bežne rozoznávaná systémom vrodenej imunity je vírusová RNA, ktorá často vstupuje do bunky pri vírusových infekciách. Keď vírusovú RNA rozoznajú molekulárne receptory, bunka reaguje spustením signalizačnej kaskády s cieľom eliminovať zdroj tohoto potenciálne nebezpečného signálu. V práci skúmame vlastnosti tejto signalizačnej kaskády danej ako sústava obyčajných diferenciálnych rovníc modelujúcich koncentrácie jednotlivých molekúl v čase po infikovaní. Naším cieľom je zjednodušenie pôvodného zložitého systému zachovajúc jeho biologické vlastnosti a vyvodenie záverov o jeho charaktere, ekvilibriách a asymptotickej stabilite.

Kľúčové slová: vrodená imunita, systémová biológia, obyčajné diferenciálne rovnice.

Abstract

MATEJOVIČOVÁ, Lenka: *Modelling innate immune response to viral infection* [Bachelor's Thesis], Comenius University in Bratislava, Faculty of Mathematics, Physics and Informatics, Department of Applied Mathematics and Statistics; Supervisor Mgr. Katarína Boďová, PhD., Bratislava, 2012, 42 p.

Co-evolution of pathogens and their hosts lead to the fact, that there are multiple immune mechanisms which recognise pathogen-associated molecular patterns. One of such molecules widely recognised by the innate immune system is viral RNA, which enters the host cell in the process of many viral infections. After recognition of the viral RNA by the receptor molecules, a signalling cascade leading to elimination of the intruder is activated. In this work we study properties of the given innate immune signalling cascade defined as a system of differential equations modelling concentrations of the molecules in time after infection. We focus on simplifying this complex system conserving the biological qualities of the model and drawing conclusions about its character, equilibria and asymptotic stability.

Key words: innate immunity, systems biology, ordinary differential equations.

Contents

Introduction

We often tend to think of size as the synonym to strength and invulnerability. However, yet an ordinary influenza infection caused by a pathogen, which is so small, that it cannot be seen even under a light microscope can cause severe problems to its host, no matter how large mass the host has.

Co-evolution of pathogens and other organisms lead to the fact, that there are multiple immune mechanisms which recognise pathogen-associated molecular patterns. In higher organisms, we can distinguish between the two types of immune response: innate and adaptive.

When a virus attempts to infect a cell, it injects its genetic information in form of a nucleic acid (RNA or DNA, depending on the type of a virus) into the host cell. In this work, we will be interested in a certain part of the innate immune response to viral infections triggered by foreign RNA recognition in a cell. Where applicable, we will use strains of Murine Norovirus (MNV) as our model virus and the data from MNV experiments.

The recognition of foreign RNA and the signalling that follows is a very complex process, that involves many species and reactions. However, better understanding of the way this process works could help us in preventing or curing the diseases caused by viral infections. The system of immune signalling has been explored in more detail e.g. in [9], [12] and [6] and many of these reaction networks have been published in on-line databases of reactions ([4], [13]).

However, pathways activated by two groups of special molecular receptors (see Background for more detail) are in literature treated separately based on structural relatedness, although there is a common trigger and significant crosstalk. Furthermore, immune signalling is a dynamic process, thus we find the exclusive use of cross-sectional data and a purely static approach inappropriate. Inspired by the Yamada's model of the JAK-STAT transduction pathway [15], the author of this work designed

a joint dynamic systems biology model [8] of innate immune response to MNV infection as a part of her summer research project.

The model is very complicated, therefore the overarching aim of this thesis is to understand how the model works (e.g. through analysis of its subsystems), test its functionality and to design simple alternative system that would give qualitatively similar results using specialised mathematical and systems biology software (MATLAB SBToolbox). We hope to explore the potential of a simplified model to describe experimental data, and to study its mathematical properties.

1 Biological background

This chapter will in more detail describe the processes and methods from life sciences and systems biology relevant to modelling of innate immune response to viral infection. In particular, we will be interested in immunology of a viral infection [2], modelling of biochemical reactions in a cell [11]. We will also introduce the nature of data selection that can be used to test and calibrate the model [3], and formulate our expectations from a functional model based on experimental results from [10] and [12].

1.1 Immunology of a viral infection

Co-evolution of pathogens and their hosts lead to development of various strategies the hosts use to fight the pathogenous agents and contrary. The strategies differ in timing, triggers and targets. In higher organisms, we can distinguish between the two types of immune response: innate and adaptive. In this work, we will focus on the innate immunity of mammals, which is less specific, yet much faster in taking an action against the pathogen than the adaptive immunity [9].

There is also a variety of pathogens using different strategies to attack the host (as mentioned in the Introduction, we will use murine norovirus (MNV) as our model virus). When an MNV attacks the cell, its genetic information in form of a ribonucleic acid (RNA) gets to the interior (cytoplasm) of a host cell. Then, the virus uses the cell's own machinery to replicate viral genetic information and to produce structural proteins which self-assembly to form new viral particles. These new particles of MNV are released into the cell's surroundings, ready to infect other cells right after the non-functional infected cell bursts open.

In mammals, normally only single-stranded RNA is present in the cytoplasm of the cells. On the other hand, viral RNA is usually present in structures specific for viruses that can be recognised by the molecule receptors of the innate immune system [9]. Recognition of such "foreign" structures inside the cytoplasm is therefore the sign of a threat to the cell and the organism as a whole and thus it leads to activation of several defence mechanisms. These typically include inflammation, apoptosis (programmed death of the infected cell) and interferon (IFN) production and release [2]. In this work,

we will focus on modelling of those pathways of the innate immune response triggered by viral RNA recognition in a cell, that lead to the type I interferon production.

In mammals, the receptors that sense viral RNA of MNV come from two different families of receptors: RIG-I-like receptors (RLRs) and toll-like receptors (TLRs). Activation of receptors leads to the activation of group of molecules called adaptors. This causes interferon regulatory factors (IRF) to dimerise (form a complex of two molecules) and enter the nucleus, where the dimers act as transcription factors, resulting in production and release of type I interferons [14]. Interferons then close the loop with a positive feedback, as they seem to up-regulate the amount of receptors in the cell [5]. Apart from this effect, the interferons also activate the JAK-STAT pathway modelled in [15], which helps to clear the infection through production of antiviral proteins.

Based on their structural relatedness, in literature the pathways activated by RLRs and TLRs are treated separately, although there is a common trigger and significant crosstalk. Therefore, the author of this work decided to design a joint systems biology model of innate immune response to MNV infection as a part of her summer research project [8]:

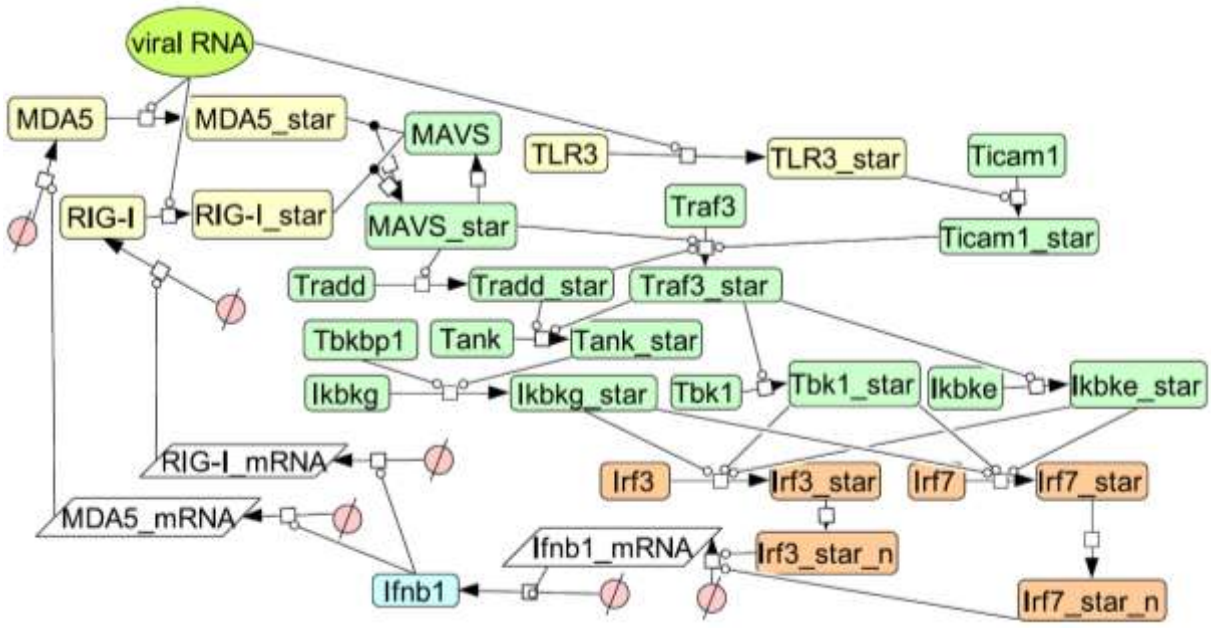

Figure 1: The complex model (CM) of innate immune response to viral RNA

Description of the model:

(Arrows denote change of state or combination of two molecules to form a complex, whereas small white circles denote catalysis of such reaction. Suffix "_star" denotes activated species, "_n" depicts location in nucleus. Pink circles denote either degraded species, or species we are not interested in, but are important in the modelling process.)

1. Viral RNA catalyses the activation of receptors (shown in yellow). It has been shown, that RIG-I like receptors (RLR) MDA5 and RIG-I and toll-like receptor (TLR) TLR3 are involved in innate immune response to MNV in mice [6], [9].
2. Activated receptors contribute to signalling through adaptors (shown in green) in different ways. There is an interconnection of RLR and TLR signalling in proteins Traf3 and Tank.
3. Final components of the adaptor signalling catalyse interferon regulatory factors (IRFs) activation. Particularly Irf3 and Irf7 were shown to be involved in type I interferon production pathway [4].
4. Activated IRFs are transferred to the nucleus, where they act as transcription factors [4], which means they catalyse the production of type I interferon mRNA (Ifnb1_mRNA).
5. Back in the cytoplasm, the Ifnb1_mRNA is translated into type I interferon Ifnb1 (shown in blue).
6. Type I interferons are shown to up-regulate RLRs [5] and the loop is complete.

While looking at this model, we should be aware, that it is just a simplification and it can be rather incomplete. The reasons can be both our trying to keep only relevant species and reactions from the very complicated published networks [4], [13] (as we are dealing with quite a specific problem in immune signalling) and the possible incompleteness of the knowledge about the innate immunity response as such (some of the involved molecules might not even be known yet).

1.2 Modelling of biochemical reactions in a cell

Once we have the idea of reactants and reactions in the system, we could be interested in kinetics of the reactions. There are two basic types of kinetics: Michaelis-Menten kinetics and mass action kinetics.

Inspired by Yamada et al. in [15], we chose simple mass action kinetics, where the rate of the reaction relates directly to the concentrations of its reactants as described in [11].

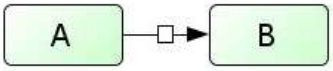

Figure 2: Simple state transition

Thus the rate of simple irreversible state transition (Figure 2) would be $\frac{dB}{dt} = kA$, where X stands for the concentration of species X and k is the rate constant for this reaction. If the state transition was reversible, then the rate of the reaction would be characterised by

$$\frac{dB}{dt} = k_f A - k_b B, \tag{1}$$

where k_f is a rate constant for the forward and k_b for the backward reaction. Since we assume conservation of the sum $A + B$, the rate of change of A concentration would be simply the opposite:

$$\frac{dA}{dt} = -\frac{dB}{dt} = -k_f A + k_b B. \tag{2}$$

In Figure 3 there is a bimolecular reaction (heterodimer formation), which means that the two different molecules (A, B) combine to form a complex (C).

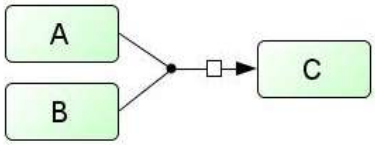

Figure 3: Bimolecular reaction

The rate of C production in this reversible reaction would be then

$$\frac{dC}{dt} = k_f AB - k_b C. \tag{3}$$

Whereas the rate of change in reactant concentrations would differ from the above only by a minus sign:

$$\frac{dA}{dt} = \frac{dB}{dt} = -\frac{dC}{dt} = -k_f AB + k_b C. \tag{4}$$

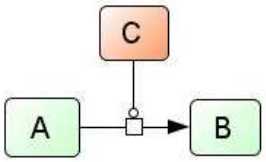

Figure 4: Catalysis of simple state transition

If the reaction of a state transition was catalysed by a species C (Figure 4), then the rate of the reversible reaction would be

$$-\frac{dA}{dt} = \frac{dB}{dt} = k_f AC - k_b B. \quad (5)$$

We need to be aware that k_f in simple state transition and k_f in catalysed state transition and bimolecular reaction differ in units.

1.3 Model versus experiment

Once we have a model with species, reactions and kinetics, we would like to test its functionality. In this part of the Background we would like to discuss the link between our model and reality.

Murine norovirus is a virus from Caliciviridae family causing infections in mice. It is very close to Human Norovirus (HuNV), which causes increasingly frequent massive outbreaks throughout the world. Although the HuNV infections are seldom lethal and only take a few days, outbreaks typically result in significant economic loss and closures of hospitals (nursing homes, kindergartens, etc.) [9].

It is believed, that with better knowledge of the way immune system responds to HuNV, the outbreaks could be handled more efficiently. However, it is complicated to culture HuNV and conduct a research on this type of norovirus. Therefore, the data from experiments on strains of MNV are used [3].

MNV is capable of causing an infection in several types of cells, particularly cells of gastro-intestinal system and innate immunity cells. As there is a widely known working cell-culture system for the latter types of cells and they are also capable of significant response to MNV, most of the experimental data available come from the research on the cells of innate immunity, namely bone marrow – derived macrophages (BMMs).

Therefore, when speaking about response of "cells" in the modelling process, we usually refer to response of these BMMs.

BMMs used in the experiments can either come from cell cultures immortalized by a suitable mutation and can therefore divide "forever" (actually, they accumulate mutations all the time they are left to divide, therefore the time of proper use of such cells is limited), or they are cultured on specific media from pluripotent cells from the bone marrow of mice. Since it involves less animal sacrifice, working with immortalised forms is sometimes preferred to experiments with pluripotent cells, although the latter seems to better reflect the reality.

Experiment

To measure the response of a cell, data from published micro-array experiments were used. This means, that in each time point, the amount of RNA needed specifically to produce particular protein molecule is measured. Micro-array data are used, because it is cheaper than measuring the same number of protein species (these data are obtainable from public databases) and there is still a good correlation between the amount of that specific RNA and its protein. The experiments involve:

1. *Setting up an appropriate tissue culture.*
   BMMs are cultured in vitro. This type of cells sticks to the bottom of the vessel, therefore enough time should be allowed for the cells in solution to stick to the bottom before an experiment starts.
2. *Triggering a response we would like to measure.*
   A trigger in form of chemical, or infectious agent is added on the top of the cell culture. In our case, synthetic RNA called poly(I:C) and type I interferons were used in different experiments to activate different stages of the examined signalling system.
3. *RNA release and stabilisation in the defined time points.*
   Using chemicals, the RNA is extracted from the cells in the defined time points. Because RNA is degraded easily, it needs to be stabilised by specific chemical preparations.
4. *Setting up the chips*
   The sample with pieces of stabilised RNA is injected into the chip. Inside the chip, there is a specific slot for each measured sequence of RNA, which contains a compatible molecule binding that particular RNA in the slot. Thus, for each slot, there is a specific

RNA sequence fixed inside. The amounts of different sequences "trapped" in different slots may differ resulting from different amounts of those particular sequences in the original solution after release and fixation. For each time point one such chip is made.

5. *Machine analysis of the RNA amounts.*

   The micro-array machine is capable of defining the amounts of RNA in the individual slots in artificial units (typically fold change), relative to the standard amounts of reference types of RNA in the sample. This way, we can say, whether a certain type of molecule coded in a specific RNA found in the sample was up-regulated, or down-regulated compared to its usual amounts.

1.3.1 Poly(I:C) experiment

Addition of the pure double-stranded RNA (dsRNA) typical for MNV infections is crucial in the first stages of building a model, because there can be other substances interacting with the signalling pathway present in the actual virus. For this purpose, we use synthetic double-stranded RNA called poly(I:C), which is widely used because of the similar response it triggers in cells when compared to MNV infections.

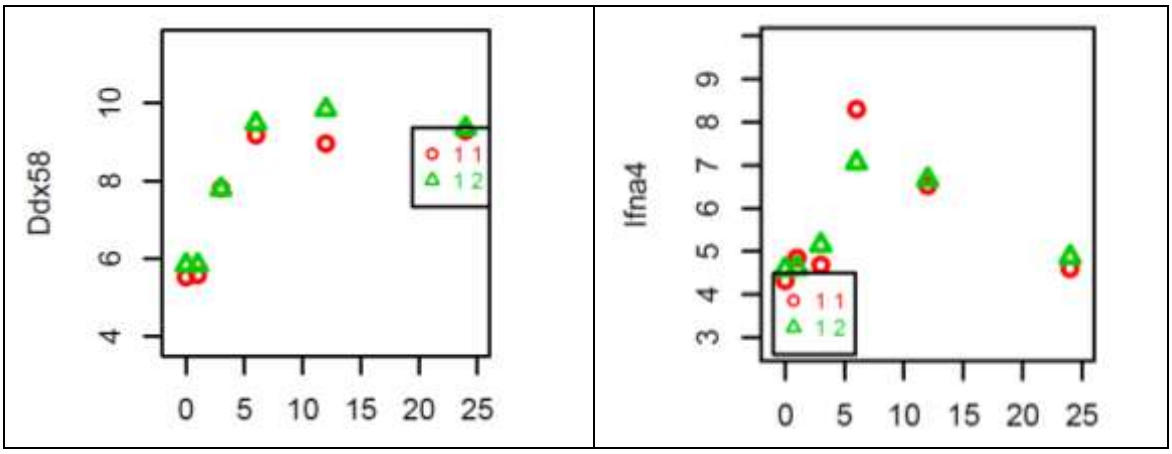

Figure 5: Poly(I:C) experiment.

Typical graphs for change in amounts (y-axis, in fold change) of receptor (Ddx58) and type I interferon (Ifna4) in time (x-axis, in hours) after addition of poly(I:C) to the BMM culture. Red circles and green triangles represent two BMM samples (from two separate animals).

After the poly(I:C) is added to the cell culture, it takes some (presumably short, yet unknown) time to enter the cells, so that it can be recognised by the receptors and trigger the examined signalling pathway.

1.3.2 IFN pulse experiment

To verify the credibility and versatility of the activation signalling model like ours, we can sometimes use data from activation of its different parts. The original model is supposed to respond to viral RNA with a production of type I interferons (IFN), which close the loop with up-regulation of receptors, speeding up the signalling system in presence of viral RNA, producing more IFNs, etc.

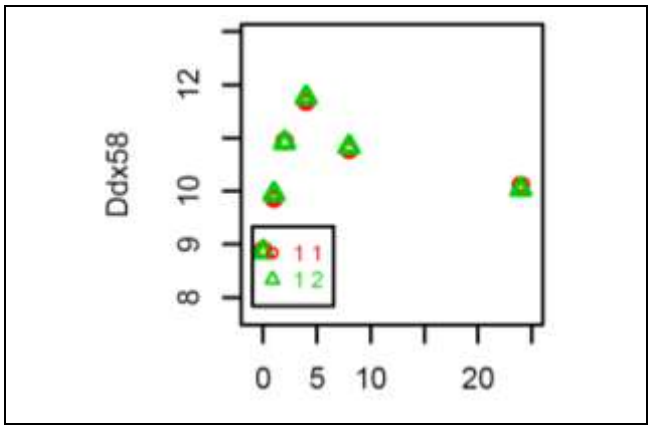

Figure 6: IFN pulse experiment.

Typical graph for change in amounts (y-axis, in fold change) of receptor (Ddx58) in time (x-axis, in hours) after addition of one shot IFN to the BMM culture. Red circles and green triangles represent two BMM samples (from two separate animals).

Therefore, to the single shot pulse of IFNs added to the system, it reacts with steep increase in receptor numbers. Followed by slow decrease resulting e.g. from IFN and RNA degradation, as there is no viral RNA present to activate the signalling pathway and keep the amounts higher.

2 The complex model (CM)

In this chapter we will make an attempt to analyse the qualities of the given complex model described in 1.1. Because the given CM is very complicated, we had to find a way to reduce the complexity of the problem and thus we chose to decompose the CM into its functional subsystems. In particular, we will pay attention to most incomprehensible subsystem of the CM – the system of adaptors.

2.1 Adaptors

The adaptors form the most complicated subsystem of the CM. The role of group of adaptor molecules (or just "adaptors") is to transmit the signal from receptors to interferon regulatory factors (IRFs).

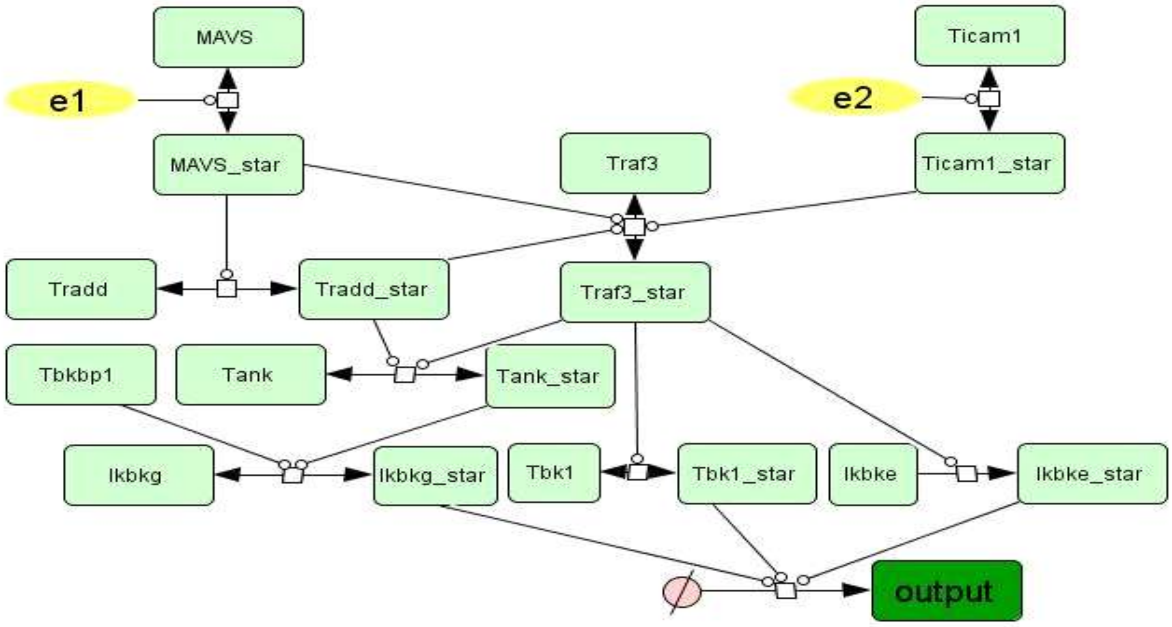

Figure 7: System of adaptors is a subsystem of the original model

Description of the model:

1. To acknowledge that we have signal from two types of receptors (RLRs and TLRs), we have two types of signal ($e1$, $e2$) in yellow ellipses.
2. There is an activation chain of reactions, where an activated molecule of a particular type of adaptor is needed to catalyse (small white circle) an activation of another type of adaptor molecule.
3. Activated form of a certain type of molecule is shown as "$\_star$" (or later with a subscript: $molecule_{star}$).

4. All the activation reactions are reversible, but no catalysts are needed for the reverse reactions.
5. Molecule $Tbkbp1$ acts as a catalyst only and the model does not allow for change in its level.
6. To explore the types of activation signal we can get from the system of adaptors, a fictive molecule of "$output$" was created (shown in dark green), which is modelled as a linear combination of $Ikbkg\_star$, $Tbk1\_star$ and $Ikbke\_star$.

The system of differential equations describing the subsystem of adaptors is as follows:

$$\frac{d(MAVS)}{dt} = -e_1 * MAVS * k_{1f} + MAVS_{star} * k_{1b} \quad (6)$$

$$\frac{d(Ticam1)}{dt} = -e_2 * Ticam1 * k_{2f} + Ticam1_{star} * k_{2b} \quad (7)$$

$$\frac{d(Traf3)}{dt} = -Ticam1_{star} * MAVS_{star} * Traf3 * Tradd_{star} + Traf3_{star} * k_{3b} \quad (8)$$

$$\frac{d(Tradd)}{dt} = -Tradd * MAVS_{star} * k_{4f} + Tradd_{star} * k_{4b} \quad (9)$$

$$\frac{d(Tank)}{dt} = -Tradd_{star} * Traf3_{star} * Tank * k_{5f} + Tank_{star} * k_{5b} \quad (10)$$

$$\frac{d(Ikbkg)}{dt} = -Tbkbp1 * Tank_{star} * Ikbkg * k_{6f} + Ikbkg_{star} * k_{6b} \quad (11)$$

$$\frac{d(Tbk1)}{dt} = -Traf3_{star} * Tbk1 * k_{7f} + Tbk1_{star} * k_{7b} \quad (12)$$

$$\frac{d(Ikbke)}{dt} = -Ikbke * Traf3_{star} * k_{8f} + Ikbke_{star} * k_{8b} \quad (13)$$

Mass conservation of each type of molecule X (either activated or not) holds, i.e. $X + X_{star} \equiv constant$. Thus, activated molecules (shown as molecule$_{star}$) have the same rate as non-active forms, but with the minus sign ($\frac{dX_{star}}{dt} = -\frac{dX}{dt}$ at all times $t > 0$, for all molecules X).

As most of the rate constants k and initial conditions values are not known, we usually run the simulations with a common value for most of the parameters and also the same

values for most initial concentrations of non-activated molecules and zero concentrations of activated molecules.

2.2 Equilibrium

In equilibrium, the concentrations of molecules do not change in time, hence values of all of the expressions (6) to (13) are equal to zero.

From putting (6) equal to zero in equilibrium we have

$$MAVS^e_{star} * k_{1b} = e_1 * MAVS^e * k_{1f} \tag{14}$$

where superscript *e* denotes the concentration of a molecule in an equilibrium.

Let us denote the ratio $\frac{k_{if}}{k_{ib}} = K_i$ for all i = 1, 2, ...8. Then, assuming that the sum of each molecule and its activated form ($molecule_{star}$) concentrations remains constant ($S_{molecule}$) with the time, we have:

$$MAVS^e = \frac{S_{MAVS}}{1 + e_1 * K_1} \tag{15}$$

$$MAVS^e_{star} = \frac{S_{MAVS} * e_1 * K_1}{1 + e_1 * K_1} \tag{16}$$

and similarly:

$$\begin{pmatrix} Ticam1^e_{star} \\ Traf3^e_{star} \\ Tradd^e_{star} \\ Tank^e_{star} \\ Ikbkg^e_{star} \\ Tbk1^e_{star} \\ Ikbke^e_{star} \end{pmatrix} = \begin{pmatrix} \frac{S_{Ticam1} * e_2 * K_2}{1 + e_2 * K_2} \\ \frac{S_{Traf3} * K_3 * Ticam1^e_{star} * MAVS^e_{star}}{1 + Ticam1^e_{star} * MAVS^e_{star} * K_3} \\ \frac{S_{Tradd} * K_4 * MAVS^e_{star}}{1 + MAVS^e_{star} * K_4} \\ \frac{S_{Tank} * K_5 * Tradd^e_{star} * Traf3^e_{star}}{1 + Tradd^e_{star} * Traf3^e_{star} * K_5} \\ \frac{S_{Ikbkg} * K_6 * Tank^e_{star} * Tbkbp^e}{1 + Tank^e_{star} * Tbkbp^e * K_6} \\ \frac{S_{Tbk1} * K_7 * Traf3^e_{star}}{1 + Traf3^e_{star} * K_7} \\ \frac{S_{Ikbke} * K_8 * Traf3^e_{star}}{1 + Traf3^e_{star} * K_8} \end{pmatrix} \tag{17}$$

Then, stating that $output$ is a linear combination of the three output molecules ($Ikbke, Tbk1$ and $Ikbkg$), in an equilibrium we have:

$$output^e = c_1 * Ikbke^e_{star} + c_2 * Tbk1^e_{star} + c_3 * Ikbkg^e_{star} \quad (18)$$

where c_1, c_2 and c_3 are the weights of respective molecules in their linear combination $output$. Using the equilibrium formulas:

$$output^e = c_1 \frac{S_{Ikbke} K_8 Traf3^e_{star}}{1 + Traf3^e_{star} K_8} + c_2 \frac{S_{Tbk1} K_7 Traf3^e_{star}}{1 + Traf3^e_{star} K_7} + c_3 \frac{S_{Ikbkg} K_6 Tank^e_{star} Tbkbp^e}{1 + Tank^e_{star} Tbkbp^e K_6} \quad (19)$$

Which can be extended further (showing $Ticam1^e_{star}$ as T, $MAVS^e_{star}$ as M and S_{Traf3} as S):

$$c_1 \frac{S_{Ikbke} K_8 \frac{S * K_3 * T * M}{1 + T * M * K_3}}{1 + \frac{S * K_3 * T * M}{1 + T * M * K_3} * K_8} + c_2 \frac{S_{Tbk1} K_7 \frac{S * K_3 * T * M}{1 + T * M * K_3}}{1 + \frac{S * K_3 * T * M}{1 + T * M * K_3} * K_7} + c_3 \frac{S_{Ikbkg} K_6 \frac{S_{Tank} K_5 \frac{S_{Tradd} * K_4 * M}{1 + M * K_4} * \frac{S * K_3 * T * M}{1 + T * M * K_3}}{1 + \frac{S_{Tradd} * K_4 * M}{1 + M * K_4} * \frac{S * K_3 * T * M}{1 + T * M * K_3} * K_5} * Tbkbp^e}{1 + \frac{S_{Tank} K_5 \frac{S_{Tradd} * K_4 * M}{1 + M * K_4} * \frac{S * K_3 * T * M}{1 + T * M * K_3}}{1 + \frac{S_{Tradd} * K_4 * M}{1 + M * K_4} * \frac{S * K_3 * T * M}{1 + T * M * K_3} * K_5} * Tbkbp^e * K_6} \quad (20)$$

Although the formula for equilibrium output $output^e$ seems to be complex, it does not reflect the rate of convergence to this equilibrium in any way.

2.3 Behaviour

As we can notice, there are two pathways of the signal transduction, which act on two distinct time scales. The "faster" one, "fed" by input $e2$ and going through $Ticam1$ and $Traf3$ straight to molecules interacting with IRFs ($Tbk1$, $Ikbke$), whereas the second, "slower" pathway, "fed" by input $e1$ going through $MAVS$, $Tradd$ and $Tank$ it takes one step more to reach the final $Ikbkg$.

Having these two pathways of signal transmission with different numbers of steps, we could expect, that the behaviour of contributions to output from respective pathways can differ in terms of the time scales. Although the graphs of output were typically just simple saturation curves like blue and red lines (Figure 8) our intuition was proven right graphically using coefficients slowing down the "slower" pathway and speeding up the faster one.

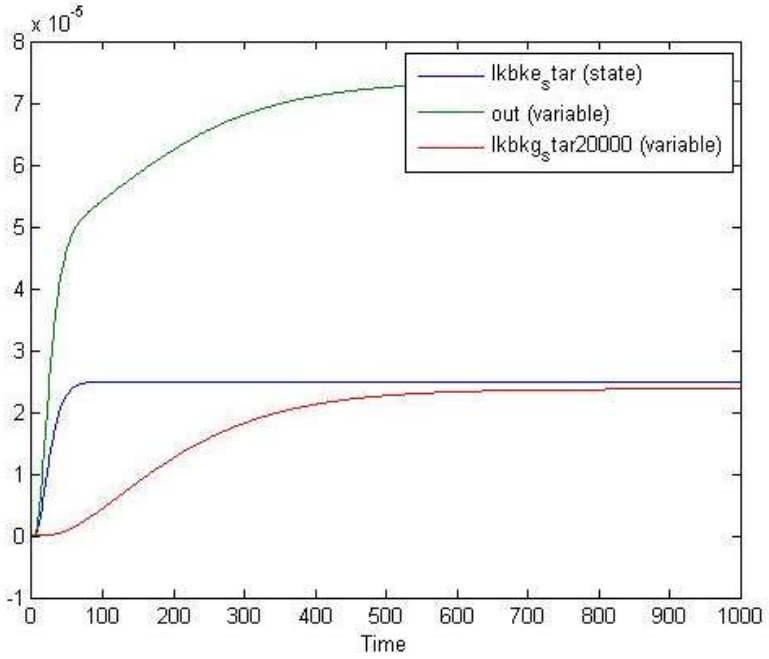

Figure 8: Two time scales in output and their combination

Green curve in the picture denotes the output, which is the sum of $Ikbke_{star}$, $Tbk1_{star}$ (two blue lines) and 20 000 times $Ikbkg_{star}$ (red line) in this case. (Because of the impact of coefficient values on concentrations described in 2.3.1, the concentration of $Ikbkg_{star}$ was approximately 2*10^{-5} smaller than those of $Ikbke_{star}$ and $Tbk1_{star}$, so we had to multiply it to make the effect of the slower branch visible in the linear combination.) We can see that at first, the green curve denoting the output rises quickly, adopting the behaviour of the blue line and only later it adopts the mild growth of the slower branch behaviour, shown in red.

The difference in time scales and ordinal change in the equilibrium concentration can be explained by the choice of coefficients k_f and k_b , and demonstrated by the following simple example.

2.3.1 Example

Let us have this simple example of state transition between molecules A and B, which can be described by the following differential equations:

$$\frac{dB}{dt} = k_{1f}A - k_{1b}B \tag{21}$$

$$\frac{dA}{dt} = -\left(k_{1f}A - k_{1b}B\right) \tag{22}$$

And the same type of reaction between molecules C and D:

$$\frac{dD}{dt} = k_{2f}C - k_{2b}D \tag{23}$$

$$\frac{dC}{dt} = -\left(k_{2f}C - k_{2b}D\right) \tag{24}$$

Setting rates constants for first reaction $k_{1f} = k_{1b} = 1$ and constants for second reaction $k_{2f} = k_{2b} = 0.1$, and identical initial conditions $A(0) = C(0) = 1$ and $B(0) = D(0) = 0$ we can see, that the second reaction runs slower and the equilibrium is achieved later, however at the exact same values:

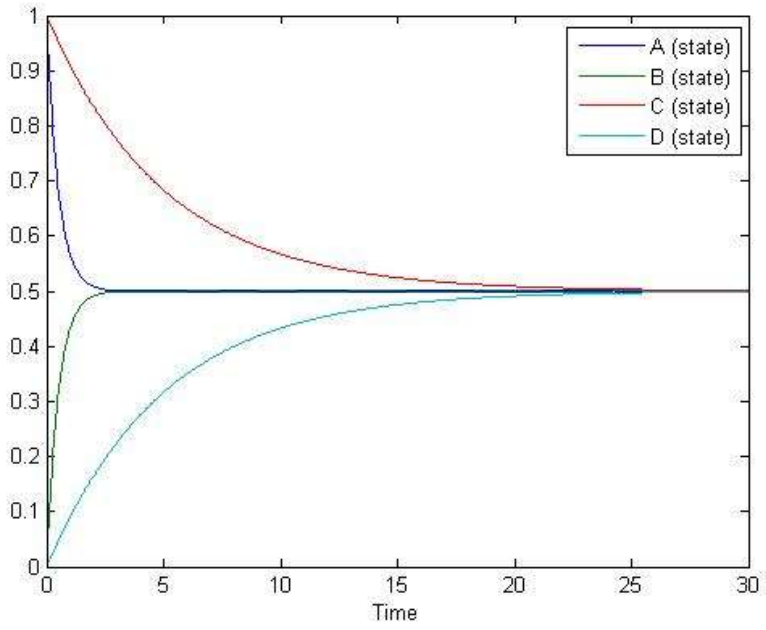

Figure 9: Difference in rate of convergence to equilibrium for reactions with higher (A to B) and lower (C to D) rate constants

If we change the ratio of the forward and backward reaction constants ($\frac{k_{if}}{k_{ib}}$), the equilibrium concentrations of the two molecules participating in the reaction will change.

It is known, that the equilibrium concentrations (A^e, B^e) of the two molecules participating in a reaction with simple mass action kinetics is determined by the ratio of the forward and backward reaction constants ($\frac{k_{1f}}{k_{1b}} = K_1$), and sum of the reacting

species concentrations (S) [11]. The reason for it is that in equilibrium, the change of concentrations is equal to zero, hence

$$\frac{dB}{dt} = k_{1f}(S - B^e) - k_{1b}B^e = 0. \tag{25}$$

Then it follows:

$$B^e = \frac{S\frac{k_{1f}}{k_{1b}}}{1 + \frac{k_{1f}}{k_{1b}}} = \frac{S\,K_1}{1 + K_1} \tag{26}$$

$$A^e = \frac{S}{1 + \frac{k_{1f}}{k_{1b}}} = \frac{S}{1 + K_1} \tag{27}$$

□

Setting $k_{2f} = 1$ and $k_{2b} = 2$ and we have $C^e = \frac{2}{3}$, $D^e = \frac{1}{3}$.

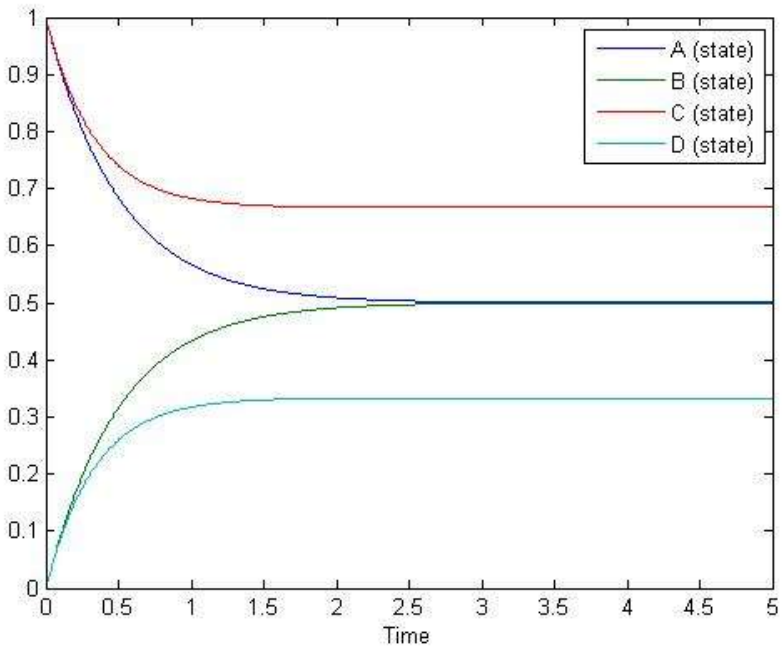

Figure 10: Difference in position of the equilibrium for reactions with different ratio of forward and backward reaction rate constants

2.4 CM: summary

Despite the high level of model complexity, the obtainable results are relatively simple. For example, from the subsystem of adaptors, we typically get an S-shaped saturation curve as the time-course simulation for the concentration of $output$. The most complex result would be a linear combination of three of such lines, which can exhibit signs of different timescales (Figure 8). Thus, since in this stage of modelling there is no obvious added value of having seventeen interacting species instead of two, the simplification of the CM seems to be a straightforward and a logical thing to do.

3 The “simple” model (SM)

In this chapter we focus on simplifying the complex system (CM introduced in 1.1) conserving the expected biological qualities of the model and drawing conclusions about its character, equilibria and linear stability. Especially, the number of reacting species in the original model will be reduced only into its intuitive subsystems (receptors, adaptors and interferons) with their activated forms and simple reactions among them.

3.1 Introduction of the SM

In this “simple” model, we made an attempt to make the number of species, interactions and their complexity as low as possible while still maintaining the expected biological qualities as described in Chapter 1 so that it makes sense to interpret the results in biological terms.

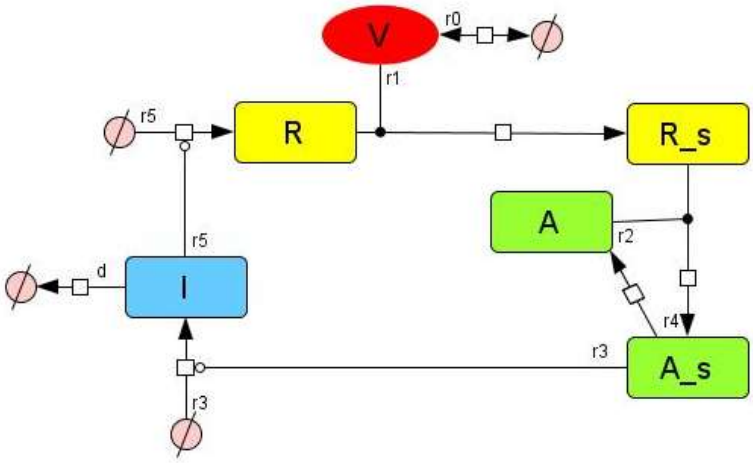

Figure 11: The "simple" model (SM)

Description of the model:

(Arrows denote state transition or combination of two species to form a new species, whereas small white circles denote catalysis of a reaction. Suffix “_s” denotes activated form of a species. Pink circles denote either degraded species, or species we are not interested in, but are important in the modelling process.)

1. In reaction labelled *r0*, the viral RNA (V, shown in red) can be replicated ($k_0 > 0$) or degraded ($k_0 < 0$) with rate depending on its concentration.

2. In reaction labelled *r1* viral RNA (V) combines with a generic receptor (R, shown in yellow) to form an activated receptor (R_S).
3. This activated receptor $R_S$combines with a generic adaptor (A, shown in green) to form an activated adaptor (A_S) in reaction *r2*, with no way of recycling receptors or V.
   (Together with $k_0 < 0$ option, these are the only two ways in which the viral RNA can be removed from a cell in this model.)
4. The activated adaptors A_S then act as catalyst, presence of which is necessary in interferon (I, shown in blue) production denoted by the reaction labelled *r3*, until they are deactivated and recycled back to become adaptor molecules again in *r4*.
5. Since the receptors are used up in the process of recognition and binding V, there is a necessity to produce new receptors during the infection. This happens in reaction *r5*, catalysed by interferons (I).
6. Interferons degrade (or leave the cell interior in other ways) with the rate directly proportionate to their concentration in the reaction labelled d.

Considering that the sum of adaptor (A) and activated adaptor (A_S) concentrations is constant at all times ($A + A_S = A_0$), the model can be described by the following differential equations:

$$\frac{dV}{dt} = k_0 V - k_1 VR \tag{28}$$

$$\frac{dR_S}{dt} = k_1 VR - k_2 (A_0 - A_S) R_S \tag{29}$$

$$\frac{dA_S}{dt} = k_2 (A_0 - A_S) R_S - k_3 A_S \tag{30}$$

$$\frac{dI}{dt} = k_4 A_S - dI \tag{31}$$

$$\frac{dR}{dt} = k_5 I - k_1 VR \tag{32}$$

Constraints and assumptions:

1. In this model, the sum of adaptor and activated adaptor concentrations is constant at all times ($\mathrm{A(t)} + \mathrm{A_S(t)} = \mathrm{A_0}$, for all times t).
2. All of the constants $\mathrm{k_1}$ to $\mathrm{k_5}$, d and $\mathrm{A_0}$ are positive numbers.
3. In this model we assume that in time $\mathrm{t} = 0$ there are no activated molecules ($\mathrm{R_S(0)} = \mathrm{A_S(0)} = 0$).
4. At all times, concentrations of all of the species are non-negative.

Constraints 1. and 4. together define the region $\mathfrak{C}$, which is the space of all biologically feasible combinations of species concentrations (and is a domain of the SM):

$$\mathfrak{C} = \{(V, R_S, A_S, I, R)^T \subset \mathbb{R}^5 | \, V, R_S, I, R \geq 0 \; and \; 0 \leq A_S \leq A_0\} \qquad (33)$$

3.2 Behaviour

Observing the behaviour of the model we can state, that with particular sets of parameters and initial conditions, for example

$$\begin{pmatrix} k_0 \\ k_1 \\ k_2 \\ k_3 \\ k_4 \\ k_5 \\ d \end{pmatrix} = \begin{pmatrix} 0 \\ 0.1 \\ 0.1 \\ 0.1 \\ 0.1 \\ 0.1 \\ 0.01 \end{pmatrix}, \quad \begin{pmatrix} V \\ R_S \\ A_S \\ I \\ R \end{pmatrix}_{t=0} = \begin{pmatrix} 0.1 \\ 0 \\ 0 \\ 0 \\ 0.1 \end{pmatrix}, \qquad A_0 = 0.1 \qquad (34)$$

the model manifests the required qualities when the simulations are compared to data from the "poly (I:C)" experiment (Figure 5).

Setting the $V(0) > 0$, $I(0) = 0$ and the $k_0 = 0$, we should model the conditions from the poly (I:C) experiment, where a certain amount of foreign, double-stranded RNA (hence $V(0) > 0$) can be recognised, but it cannot replicate itself (hence $k_0 = 0$).

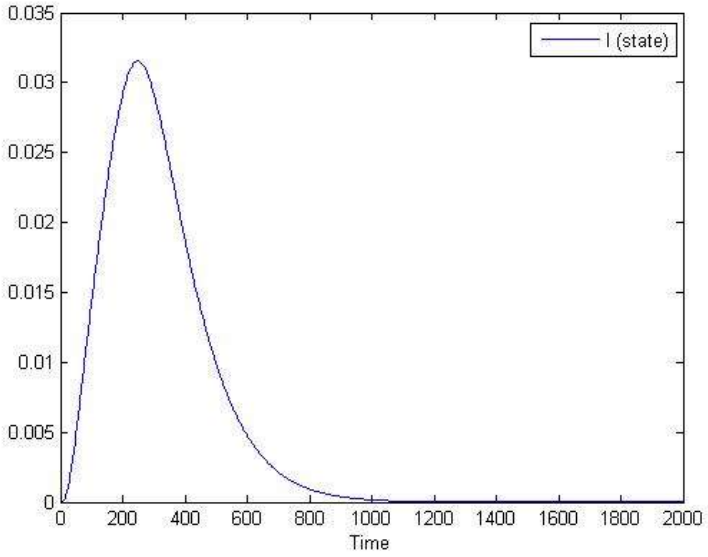

Figure 12: Simulated interferon concentration in time.

Both time on the x-axis and concentration on the y-axis are in artificial units.

In this picture, we can see, that our expectations about the behaviour of interferon (I) concentration can be satisfied. First, the concentration of I rises steeply, peaks at approximately $t = 250$ time units and then it decreases.

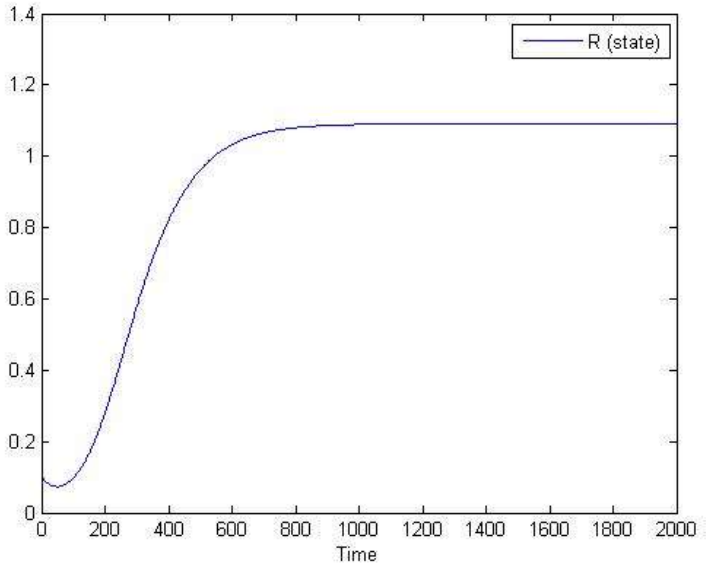

Figure 13: Simulated receptor concentration in time.

Both time on the x-axis and concentration on the y-axis are in artificial units.

With the same set of parameters and initial values, the expectations about receptor (R) concentration can be satisfied: first, there is small decrease in R due to binding the RNA before the whole system feeding back to the receptors begins to work. Then it rises steeply to reach a plateau.

Setting the $V(0) = 0, I(0) > 0$, we should model the conditions from the "IFN pulse" experiment, where a certain amount of interferon is introduced to the cells (hence $I(0) > 0$), but no viral RNA, nor its equivalent is present ($V(0) = 0$).

Apparently, SM is too simple to explain the data from the "IFN pulse" experiment (Figure 10). The reason for this is that the visible decrease in receptor (R) level could only be achieved in SM by receptors binding viral RNA. However, modelling the conditions for "IFN pulse" experiment, we set the $V(0) = 0$ and to make such decrease possible, new reactions would have to be added (for example spontaneous concentration-dependent receptor degradation).

3.3 Equilibrium

In an equilibrium, the concentrations of molecules do not change in time, hence values of all of the expressions (28) to (32) are equal to zero.

First common sense equilibrium would be when $V^e = 0$ (hence the name "zero" equilibrium). Concentrations in this equilibrium are denoted with an additional superscript: $molecule^{e0}$. The receptor molecules have nothing to bind, therefore there are no activated receptors, nor adaptors and there are no reactions running in the "simple" model. The "zero" equilibrium concentrations are as follows:

$$(V^{e0}, R_S^{e0}, A_S^{e0}, I^{e0}, R^{e0}) = (0, 0, 0, 0, R^{e0}) \tag{35}$$

Note: It is not possible to express any constraints for the "zero" equilibrium concentration of receptors (R^{e0}), because in differential equations (28) to (32), R^{e0} is only found in a product with V^{e0}, which is always equal to zero ($V^{e0}R^{e0} = 0$) if $V^e = 0$.

In all the other ("non-zero") equilibria, $V^e \neq 0$. Putting (28) equal to zero, for equilibrium concentration of receptors (which is R^e), where $V^e \neq 0$ we have:

$$R^e = \frac{k_0}{k_1} \tag{36}$$

With use of (35), the "non-zero" equilibrium concentrations are as follows:

$$(V^e, R_S^e, A_S^e, I^e, R^e) = \left(V^e, \frac{k_0 V^e}{k_2\left(A_0 - \frac{k_0 V^e}{k_3}\right)}, \frac{k_0}{k_3}\ V^e, \frac{k_0}{k_5} V^e, \frac{k_0}{k_1} \right) \tag{37}$$

with a constraint

$$\frac{k_4 k_5}{k_3 d} = 1 \tag{38}$$

The necessary condition (38) for "non-zero" equilibrium can be interpreted as a balance between excitation (rate constant of IFN production k_4 and receptor production k_5) and damping (rate constant of IFN degradation d and adaptor deactivation k_3) the "simple"

model. Since all of the model processes are stopped if viral RNA is not present in the system, the condition is not necessary for existence of the "zero" equilibrium.

Note: As there was not enough information in the system of differential equations, the equilibrium concentrations could not be expressed in the explicit form. Therefore, we chose V^e as the reference value, which is needed to express all the other equilibrium concentrations.

3.4 Host vs. virus

Using this "simple" model, the ability of host cell fighting the viral RNA can be observed and some marginal values of parameters, or initial conditions can be derived.

For example, the marginal relationships between the parameter values could be studied. If k_0 is low enough in comparison with other parameter and initial conditions values, the viral RNA can be degraded (and infection cleared) in a reasonable amount of time:

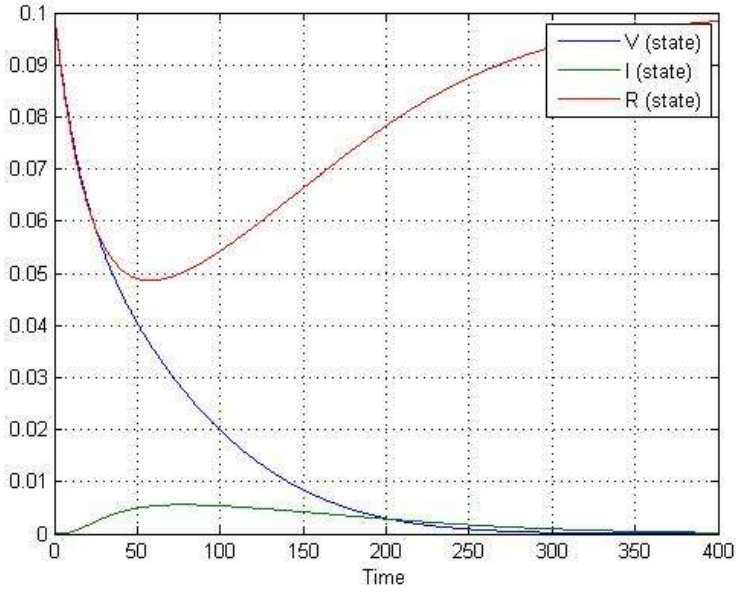

Figure 14: Viral RNA is degraded, because its replication was too slow

This result was achieved with values

$$\begin{pmatrix} k_0 \\ k_1 \\ k_2 \\ k_3 \\ k_4 \\ k_5 \\ d \end{pmatrix} = \begin{pmatrix} 0.001 \\ 0.3 \\ 0.15 \\ 0.1 \\ 0.1 \\ 0.1 \\ 0.1 \end{pmatrix}, \quad \begin{pmatrix} V \\ R_S \\ A_S \\ I \\ R \end{pmatrix}_{t=0} = \begin{pmatrix} 0.1 \\ 0 \\ 0 \\ 0 \\ 0.1 \end{pmatrix}, \; A_0 = 0.1.$$

However, if the k_0 rate constant of the viral replication is too high, it can defeat the immune system:

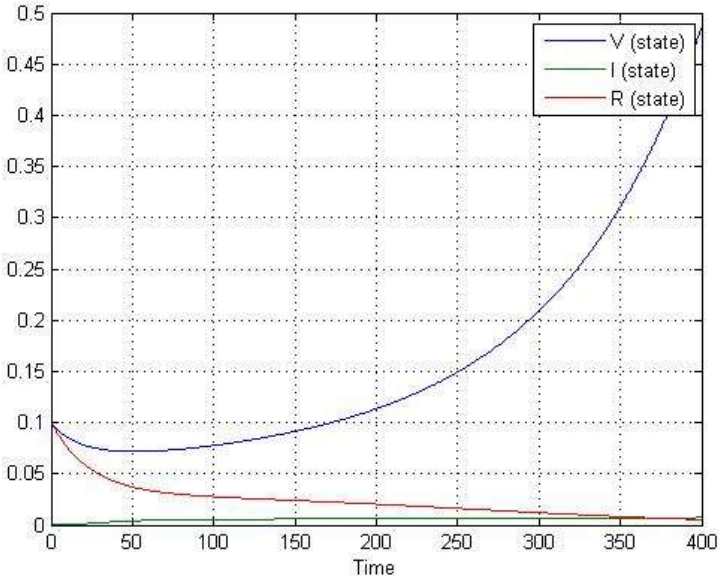

Figure 15: Immune system defeated, viral RNA replicated too fast

These results were achieved with values

$$\begin{pmatrix} k_0 \\ k_1 \\ k_2 \\ k_3 \\ k_4 \\ k_5 \\ d \end{pmatrix} = \begin{pmatrix} 0.011 \\ 0.3 \\ 0.15 \\ 0.1 \\ 0.1 \\ 0.1 \\ 0.1 \end{pmatrix}, \quad \begin{pmatrix} V \\ R_S \\ A_S \\ I \\ R \end{pmatrix}_{t=0} = \begin{pmatrix} 0.1 \\ 0 \\ 0 \\ 0 \\ 0.1 \end{pmatrix}, \; A_0 = 0.1.$$

And a "non-zero" equilibrium can be found experimenting with the values of parameters in numerical simulations as well:

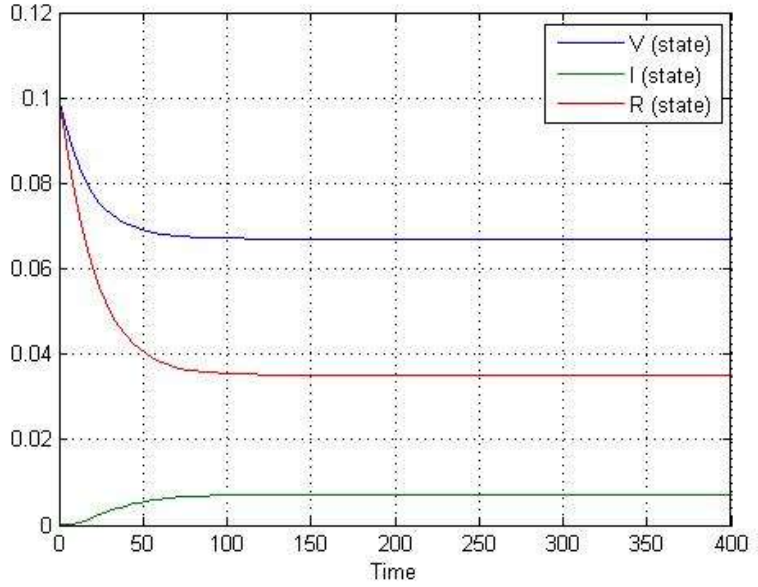

Figure 16: An example of "non-zero" equilibrium.

Concentration on y-axis and time on x-axis in artificial units.

This equilibrium was achieved using values

$$\begin{pmatrix} k_0 \\ k_1 \\ k_2 \\ k_3 \\ k_4 \\ k_5 \\ d \end{pmatrix} = \begin{pmatrix} 0.01054 \\ 0.3 \\ 0.15 \\ 0.1 \\ 0.1 \\ 0.1 \\ 0.1 \end{pmatrix}, \quad \begin{pmatrix} V \\ R_S \\ A_S \\ I \\ R \end{pmatrix}_{t=0} = \begin{pmatrix} 0.1 \\ 0 \\ 0 \\ 0 \\ 0.1 \end{pmatrix}, \qquad A_0 = 0.1$$

We can see, that the $R^e = \frac{k_0}{k_1}$ calculated earlier in this chapter is approximately satisfied. Since $k_3 = k_4 = k_5 = d = 0.1$, the condition $\frac{k_4 k_5}{k_3 d} = 1$ is satisfied in this non-zero equilibrium.

Note: Of course, that this model is assumedly too simple, but this particular analysis could be quite useful in the real-world applications. For example, the problem with norovirus is, that it stays persistent in immunodeficient individuals, which can become the source of new outbreak for the wide population in conditions suitable for the virus. However, if the individuals immunodeficient in that particular way (in SM e.g. too low k_1 resulting from mutation in receptors) favourable for norovirus could be detected and isolated from others or cured, it could help significantly with handling the norovirus outbreaks.

3.5 Asymptotic stability of the equilibrium

To explore the character of an equilibrium, we can use a Jacobi matrix for the system of differential equations (28) to (32):

$$J(V,R_S,A_S,I,R)=\begin{pmatrix} -k_1R+k_0 & 0 & 0 & 0 & -k_1V \\ k_1R & -k_2(A_0-A_s) & k_2R_s & 0 & k_1V \\ 0 & k_2(A_0-A_s) & -k_2R_s-k_3 & 0 & 0 \\ 0 & 0 & k_4 & -d & 0 \\ -k_1R & 0 & 0 & k_5 & -k_1V \end{pmatrix} \tag{39}$$

which for "zero" equilibrium ($V^e=0$) is $J^{e0}=J(V^{e0},R_S^{e0},A_S^{e0},I^{e0},R^{e0})$

$$J^{e0}=\begin{pmatrix} k_0-k_1R^{e0} & 0 & 0 & 0 & 0 \\ k_0 & -k_2A_0 & 0 & 0 & 0 \\ 0 & k_2A_0 & -k_3 & 0 & 0 \\ 0 & 0 & k_4 & -d & 0 \\ -k_1R^{e0} & 0 & 0 & k_5 & 0 \end{pmatrix} \tag{40}$$

and for "non-zero" equilibrium ($V^e\neq 0$) it is $J^e=J(V^e,R_S^e,A_S^e,I^e,R^e)$

$$J^e=\begin{pmatrix} 0 & 0 & 0 & 0 & -k_1V^e \\ k_0 & -k_2\left(A_0-\frac{k_0}{k_3}V^e\right) & \frac{k_0V^e}{A_0-\frac{k_0}{k_3}V^e} & 0 & k_1V^e \\ 0 & k_2\left(A_0-\frac{k_0}{k_3}V^e\right) & -\frac{k_0V^e}{A_0-\frac{k_0}{k_3}V^e}-k_3 & 0 & 0 \\ 0 & 0 & k_4 & -d & 0 \\ -k_0 & 0 & 0 & k_5 & -k_1V^e \end{pmatrix} \tag{41}$$

If a particular equilibrium is stable, the Jacobi matrix in that equilibrium has no positive eigenvalues [1].

J^{e0} is a triangular matrix, hence all of its eigenvalues $k_0-k_1R^{e0}$, $-k_2A_0$, $-d$, $-k_3$ and one zero can be found on the diagonal of J^{e0}. If the "zero" equilibrium is stable, J^{e0} has no positive eigenvalues. Since all of the constants k_1 to k_5 and A_0 are positive numbers, eigenvalues $-k_2A_0$, $-d$ and $-k_3$ are negative. Eigenvalue $k_0-k_1R^{e0}$ is not

positive, if $\frac{k_0}{k_1} \leq R^{e0}$. However, there is still at least one zero eigenvalue, which does not allow for standard asymptotical stability analysis based on linearization and examination of the Jacobi matrix eigenvalues.

3.6 Invariance

Some of the solutions $(V, R_S, A_S, I, R)^T \subset \mathbb{R}^5$ do make sense in real world and some of them may not. To specify the region of acceptable solutions, we defined the region $\mathfrak{C}$ in (33). All of the reactant concentrations are non-negative numbers in $\mathfrak{C}$ and the overall amount of adaptors stays conserved through the time.

In this part, we will show, that the "simple" model (SM) allows only for those trajectories with origin in region $\mathfrak{C}$, which do not leave it at any time $t > 0$. In other words, if in time $t = 0$ all of the concentrations are non-negative and the overall amount of adaptors is A_0, there is no set of circumstances, under which the concentration values would change so that they would not conform with these two requirements.

Proposition: The region $\mathfrak{C}$ is invariant with respect to the system of differential equations (28) to (32).

Proof: We will show that at any boundary of the region $\mathfrak{C}$ trajectories move towards interior of $\mathfrak{C}$ or stay at the boundary. Since at the boundary some of the conditions $V = 0, R_S = 0, A_S = 0, A_S = A_0, I = 0, R = 0$ is satisfied, we need to show that the variable defining the boundary does not cross it. We can do so using time derivatives of that particular variable, which must not be negative at the zero boundaries and must not be positive at this particular boundary: $A_S = A_0$.

For example, if we want to show, that V cannot transition into the negative numbers, we need to prove, that at the boundary, where $V = 0$, the $\frac{dV}{dt} \geq 0$ for all of the $(0, R_S, A_S, I, R)^T \subset \mathfrak{C}$ (hence the V cannot further decrease and become negative at this point).

If $V = 0 \quad \Rightarrow \quad \frac{dV}{dt} = k_0 V - k_1 V R = 0 * (k_0 - k_1 R) = 0, \ \forall \ (0, R_S, A_S, I, R)^T \subset \mathfrak{C}.$

Therefore, not only are the trajectories passing through boundary $V = 0$ staying in the region $\mathfrak{C}$, but they even stay at that particular boundary, i.e. the region

$$\left\{(V, R_S, A_S, I, R)^T \subset \mathbb{R}^5 \mid V = 0, R_S, I, R \geq 0 \; and \; 0 \leq A_S \leq A_0\right\} \subset \mathfrak{C}$$

itself is invariant with respect to the SM.

And, similarly:

if $R_S = 0$ $\Rightarrow$ $\frac{dR_S}{dt} = k_1 VR - k_2(A_0 - A_S)R_S = k_1 VR \geq 0, \; \forall \, (V, 0, A_S, I, R)^T \subset \mathfrak{C},$

if $A_S = 0$ $\Rightarrow$ $\frac{dA_S}{dt} = k_2(A_0 - A_S)R_S - k_3 A_S = k_2 A_0 R_S \geq 0, \; \forall \, (V, R_S, 0, I, R)^T \subset \mathfrak{C}.$

However, the overall amount of adaptors stays conserved ($A + A_S = A_0$) and we need non-negative concentration of A as well. Therefore we need to prove that the constraint $A_S \leq A_0$ stays conserved. Thus we need to show, that at the boundary, where $A_s = A_0$, the $\frac{dA_S}{dt} \leq 0$ for all of the $(V, R_S, A_0, I, R)^T \subset \mathfrak{C}$ (hence the A_S cannot further increase and become higher than A_0 at this point).

If $A_S = A_0$ $\Rightarrow$ $\frac{dA_S}{dt} = k_2(A_0 - A_S)R_S - k_3 A_S = -k_3 A_S \leq 0, \; \forall \, (V, R_S, A_0, I, R)^T \subset \mathfrak{C},$

if $I = 0$ $\Rightarrow$ $\frac{dI}{dt} = k_4 A_S - dI = k_4 A_S \geq 0, \; \forall \, (V, R_S, A_S, 0, R)^T \subset \mathfrak{C},$

if $R = 0$ $\Rightarrow$ $\frac{dR}{dt} = k_5 I - k_1 VR = k_5 I \geq 0, \; \forall \, (V, R_S, A_S, I, 0)^T \subset \mathfrak{C}.$

We have just shown that at any boundary of the region $\mathfrak{C}$ trajectories move towards interior of $\mathfrak{C}$ or stay at the boundary, therefore the region $\mathfrak{C}$ is invariant with respect to the system of differential equations (28) to (32).

□

Conclusions

In this work, we first understood the biological problem of innate immunity signalling in response to viral infection. We defined the field of our interest as the part of innate immunity signalling, which has not been widely studied with mathematical tools, yet it is known to be crucial for recognition and response to certain types of viral infection in mammals (such as infections with murine norovirus). We translated this biological problem into mathematical model with use of differential equations and described the ideal qualities we could expect from the model.

In the second chapter, we studied the original complex model (CM). We examined how the parameters and initial values in the model can affect the behaviour of a system and demonstrated it on a simple example. We uncovered the two communicating pathways in the subsystem of adaptors, operating on two distinct time scales and we also found out, that the complexity of the subsystem of adaptors does not add significant variability into the behaviour of the output.

The latter idea lead to the simplification of the CM, which is described and further examined in Chapter 3. The simulations of the "simple" model (SM) are compared to the experimental data and also the mathematical attributes of the model were examined. We studied the ability of system to "fight" the viral RNA depending on parameter and initial conditions values of the model and suggested applications of this approach in the real world. Inthis chapter we proved, that the domain of SM we defined on the basis of biological expectations from the model, is invariant with respect to the system of differential equations forming the SM. We found two types of equilibria in the model; "zero" equilibrium, where the equilibrium concentration of viral RNA is zero and "non-zero" equilibrium, for equilibria with non-zero concentration of viral RNA. We studied asymptotic stability of the "zero" equilibrium and found necessary condition $\frac{k_0}{k_1} \leq R^{e0}$ for the asymptotic stability of the "zero" equilibrium. However, this condition is not sufficient, because there would be still at least one zero eigenvalue found in the corresponding Jacobi matrix.

Although we did not succeed in examining the asymptotic stability through the standard procedure with Jacobi matrices, it can be achieved by other means, namely by finding a Lyapunov function of a system [7].

In the stage of the knowledge about innate immune signalling nowadays, where a lot of reaction parameters, reactions itself or even species remain unknown, we consider understanding the basic dynamics of the system crucial. Our SM could explain the experimental results from the poly(I:C) experiment, but was not complex enough to explain the data from IFN pulse experiment. This suggests, that the SM should be modified at least to meet our expectations in terms of interpreting the experimental data we already have. These modifications could include simple reactions, that make sense in biology, for example RNA or protein degradation. The "up-to-bottom" approach could make the complex model even more complex, including all possible known reactions and then use software algorithms to simplify it out and keep only the relevant species or groups of them.

Resumé

Pri niektorých vírusových infekciách sú v bunke prítomné typické štruktúry RNA (napr. dvojvláknová RNA), ktoré sú rozoznávané a vyhodnocované ako "cudzie" mechanizmami vrodenej imunity. Na takýto podnet od molekulárnych receptorov potom bunka reaguje spustením signalizačnej kaskády s cieľom eliminovať zdroj tohoto potenciálne nebezpečného signálu. V práci sa zaoberáme jedným typom takýchto signalizačných dráh aktivovaných naším modelovým vírusom, ktorý vyúsťuje do produkcie interferónov typu 1. Tieto látky zvyšujú produkciu antivírusových molekúl priamo v danej bunke, alebo po uvoľnení do medzibunkového priestoru signalizujú prítomnosť vírusu aj okolitým bunkám. Proces modelujeme pomocou sústavy obyčajných diferenciálnych rovníc. Cieľom práce je identifikovať dôležitejšie a menej dôležité prvky pri modelovaní špecifickej časti vrodenej imunitnej odpovede na vírusovú infekciu, zjednodušiť pôvodný model [8] zachovajúc biologický význam jeho jednotlivých zložiek a analyzovať vlastnosti získaného jednoduchšieho modelu.

V prvej kapitole sme zhrnuli základné poznatky z imunológie a dynamiky chemických reakcií potrebné na vytvorenie modelu. Predstavujeme súvisiace experimenty a na základe ich výsledkov formulujeme charakteristiky, ktorými by dobrý model mal disponovať. Uvádzame tu tiež pôvodný model (Figure 1).

V druhej kapitole skúmame pôvodný model a analyzujeme jeho podsystém adaptorov (Figure 7). Na jednoduchých príkladoch tu ilustrujeme vplyv výberu koeficientov rýchlostí priamej a spätnej reakcie na vlastnosti výstupu: pomer hodnôt priamej a spätnej reakcie determinuje rozdelenie koncentrácií molekúl v ekvilibriu, zatiaľčo absolútna veľkosť týchto parametrov vplýva na rýchlosť konvergencie systému k ekvilibriu. Objavili sme dve signalizačné cesty v systéme adaptorov, ktoré môžu fungovať v dvoch rôznych časových škálach a našli sme kombinácie parametrov a počiatočných podmienok na vizualizáciu týchto rôznych časových škál. Ukazuje sa, že relatívna zložitosť podsystému adaptorov nenapomáha k vysvetleniu experimentálnych dát, ani k dosiahnutiu želateľného správania modelu.

V tretej kapitole predstavujeme zjednodušený model (Figure 11) a študujeme sústavu obyčajných diferenciálnych rovníc, ktorá ho popisuje. Simulácie naznačujú, že hoci je model veľmi jednoduchý, môže stačiť na interpretáciu výsledkov niektorých typov experimentov, no pre jeho všeobecnejšie aplikácie je nutné model rozšíriť o ďalšie prvky (napr. o spontánnu degradáciu proteínov). Hodnoty jednotlivých koncentrácií v ekvilibriu sústavy obyčajných diferenciálnych rovníc vyjadrujeme pomocou rovnovážnej koncentrácie vírusovej RNA v systéme, keďže sústava neobsahuje dostatočné množstvo informácie na ich explicitné vyjadrenie. Objavili sme dva typy ekvilibrií: „nulové“ ekvilibrium bez prítomnosti vírusovej RNA a „nenulové“ ekvilibrium kde je rovnovážna koncentrácia vírusovej RNA nenulová. Asymptotická stabilita ekvilibrií je daná vlastnými hodnotami Jacobiho matice zodpovedajúcej ekvilibriám, no keďže tieto boli pre naše ekvilibriá záporné a nulové, nemožno o stabilite ekvilibrií rozhodnúť jednoznačne. Ukážeme, že systém obyčajných diferenciálnych rovníc spĺňa zmysluplný prepoklad, že biologicky relevantný stavový priestor $\mathfrak{C}$ definovaný v (33) je invariantný vzhľadom na systém.

Bibliography

[1] Brunovský, P.: *Diferenčné a diferenciálne rovnice,* text to lectures, Comenius University in Bratislava, Bratislava (2006)

[2] Chain, B. M., Playfair, J. H. L.: *Immunology at a Glance*. Wiley-Blackwell, Chichester, 2009

[3] Chettle, J.: *The impact of murine norovirus infection on the immune response and on co-infection by other enteric pathogens*, Doctoral Thesis, Department of Veterinary medicine, University of Cambridge (work in progress)

[4] Kanehisa Laboratories: *RIG-I-like receptor signaling pathway*, KEGG PATHWAY Database, available on internet (14.12.2011): http://www.genome.jp/kegg/pathway.html

[5] Kang, D. Et al.: *Expression analysis and genomic characterization of human melanoma differentiation associated gene-5, mda-5: a novel type I interferon-responsive apoptosis-inducing gene*, Oncogene 23 (2004), 1789

[6] Kato, H. et al.: *Differential roles of MDA5 and RIG-I helicases in the recognition of RNA viruses,* Nature 441 (2006), 101

[7] Lyapunov, A. M.: *Stability of Motion*, Academic Press, New-York & London, 1966

[8] Matejovičová, L. et. al.: *Modelling the Innate Immune Response to Murine Norovirus Infection.* Amgen Scholars Programme Summer project at University of Cambridge, 2011

[9] McCartney, S. A. et al.: *MDA-5 recognition of a murine norovirus*, PLoS Pathogens 7 (2008), Paper 90

[10] Olex, A. L. et al.: *Dynamics of dendritic cell maturation are identified through a novel filtering strategy applied to biological time-course microarray replicates,* BMC Immunology 11 (2010), 41

[11] Phillips, R., Kondev, J., Theriot, J.: *Physical Biology of the Cell*, Garland Science, New York, 2008

[12] Raza, S. et al.: Construction of a large scale integrated map of macrophage pathogen recognition *and effector systems*, BMC Syst Biol. 4 (2010) Paper 63

[13] REACTOME Team: *REACTOME*, Pathway database, available on internet (16.8.2011): http://www.reactome.org

[14] Takaoka, A., Hideyuki, Y.: *Interferon signalling network in innate defence*, Cellular Microbiology 8 (2006), 907

[15] Yamada, S. et al.: *Control mechanism of JAK/STAT signal transduction pathway.* Febs. Lett. 534 (2003), 190